



THE UNIVERSITY *of* EDINBURGH

Edinburgh Research Explorer

## Experimental and CFD Analysis of the Wake Characteristics of Tidal Turbines

### Citation for published version:

Gebreslassie, M, Ordonez, S, Tabor, G, Belmont, M, Bruce, T, Payne, G & Moon, I 2016, 'Experimental and CFD Analysis of the Wake Characteristics of Tidal Turbines', *International Journal of Marine Energy*, vol. 16, pp. 209–219. <https://doi.org/10.1016/j.ijome.2016.07.001>

### Digital Object Identifier (DOI):

[10.1016/j.ijome.2016.07.001](https://doi.org/10.1016/j.ijome.2016.07.001)

### Link:

[Link to publication record in Edinburgh Research Explorer](#)

### Document Version:

Peer reviewed version

### Published In:

International Journal of Marine Energy

### General rights

Copyright for the publications made accessible via the Edinburgh Research Explorer is retained by the author(s) and / or other copyright owners and it is a condition of accessing these publications that users recognise and abide by the legal requirements associated with these rights.

### Take down policy

The University of Edinburgh has made every reasonable effort to ensure that Edinburgh Research Explorer content complies with UK legislation. If you believe that the public display of this file breaches copyright please contact [openaccess@ed.ac.uk](mailto:openaccess@ed.ac.uk) providing details, and we will remove access to the work immediately and investigate your claim.



# Accepted Manuscript

Experimental and CFD Analysis of the Wake Characteristics of Tidal Turbines

Mulualem G. Gebreslassie, Stephanie O. Sanchez, Gavin R. Tabor, Michael R. Belmont, Tom Bruce, Grégory S. Payne, Ian Moon

PII: S2214-1669(16)30046-7  
DOI: <http://dx.doi.org/10.1016/j.ijome.2016.07.001>  
Reference: IJOME 118

To appear in:

Received Date: 17 July 2015  
Revised Date: 5 July 2016  
Accepted Date: 15 July 2016



Please cite this article as: M.G. Gebreslassie, S.O. Sanchez, G.R. Tabor, M.R. Belmont, T. Bruce, G.S. Payne, I. Moon, Experimental and CFD Analysis of the Wake Characteristics of Tidal Turbines, (2016), doi: <http://dx.doi.org/10.1016/j.ijome.2016.07.001>

This is a PDF file of an unedited manuscript that has been accepted for publication. As a service to our customers we are providing this early version of the manuscript. The manuscript will undergo copyediting, typesetting, and review of the resulting proof before it is published in its final form. Please note that during the production process errors may be discovered which could affect the content, and all legal disclaimers that apply to the journal pertain.

# Experimental and CFD Analysis of the Wake Characteristics of Tidal Turbines

Mulualem G. Gebreslassie<sup>☆a</sup>, Stephanie O. Sanchez<sup>c</sup>, Gavin R. Tabor<sup>b</sup>, Michael R. Belmont<sup>b</sup>, Tom Bruce<sup>d</sup>, Grégory S. Payne<sup>d</sup>, Ian Moon<sup>b</sup>

<sup>a</sup>*EiT-M, Mekelle University, Endayesus Campus, P.O. Box 231, Mekelle, Ethiopia*

<sup>b</sup>*CEMPS, University of Exeter, North Park Road, Exeter, EX4 4QF, UK*

<sup>c</sup>*Energy Systems Research Unit, Department of Mechanical and Aerospace Engineering  
University of Strathclyde, 75 Montrose Street, Glasgow, G1 1XJ*

<sup>d</sup>*Institute for Energy Systems, School of Engineering, The University of Edinburgh  
Mayfield Road, Edinburgh, EH9 3JL*

---

## Abstract

This paper investigates the accuracy of the Computational Fluid Dynamics (CFD) based Immersed Body Force (IBF) turbine modelling method for predicting the flow characteristics of a Momentum-Reversal-Lift type of tidal turbine. This empirically-based CFD model has been developed based on the actuator disc method enhanced with additional features to mimic the effect of the complex blade motion on the downstream wake, without the high computational costs of explicitly modelling the dynamic blade motion. The model has been calibrated against the flow characteristics data obtained from experiment and found to perform well, although there are few inconsistencies in the flow patterns which show some of the limitations of the IBF model compared to a full dynamic blade motion simulation. However, given the complexity and computational cost of modelling the detailed blade motion the limitations of the IBF model are acceptable and will be useful especially for optimisation of arrays of devices where there is a significant computational demand.

**Keywords:** CFD, IBF model, Experiment, wake profiles

---



---

<sup>☆</sup>Corresponding author. *Email address:* [mgg204@ex.ac.uk](mailto:mgg204@ex.ac.uk) (M.G. Gebreslassie)

## 1. Introduction

Most researchers accept that simple momentum sink zone models such as actuator disc methods are unable to generate the detailed physics of the flow produced by real turbines. However, because of their lower computational cost they are one of the few computationally realistic approaches for gaining insight into the behaviour of substantial clusters of devices. The principle of an actuator disc has been frequently utilized for modelling turbines both in experimental and computational studies. The disc acts as a momentum sink which is matched to the thrust coefficients of the turbine [1, 2]. This method has been widely used for wind turbines as documented by [3, 4]. Recently this method has been used in tidal turbines both in experiments [2] and using Computational Fluid Dynamics (CFD) techniques [5–7].

Wake profiles measured from experiment conducted by [2] using porous disc have shown reasonable agreement with actuator disc-Reynolds Averaged Navier Stokes (RANS) models in equivalent CFD simulations. However, validation of the CFD model using data measured from experimental work on simplistic disc may not be the best option to analyse fidelity of the model and to apply this model in the real turbine applications. A recent study by [8] demonstrated that the actuator disc-RANS model accurately predicts the wake of tidal turbines when compared with the wake measurements from experiment though they acknowledged that it lacks the capability to generate swirling flows and capture tip vortices.

Most of the studies showed that the accuracy of actuator disc methods in replicating the actual flow characteristics of the real turbines varied significantly. Trying to represent all types of turbine designs by a single simplistic actuator disc model may aggravate its existing drawbacks and could be one of the reasons for those inaccuracies. Thus it is crucial to adapt the method based on the details of the turbine under consideration to improve the accuracy of the models for predicting the flow characteristics.

The focus of this study is on the Momentum-Reversal-Lift (MRL) turbine designed based on a cylindrical cycloidal system where each of three blades rotates  $180^\circ$  for every full rotation of the main shaft. Details of the MRL turbine dimensions and its blade profile is shown in Figures 2 and 5. This design allows the blades to provide torque through most of the cycle in both lift and drag phases. It is this combination of both lift and drag which gives the turbine a high conversion efficiency over a wide range of operating fluid velocities. The novel aspect of the device is the combination of lift and momentum reversal (drag) that is utilised to optimise the energy extraction. It has been known since the early days of aerody-

namics that the forces on a plate held in a flowing stream consist of two orthogonal components:

1. Lift which acts perpendicularly to the flow direction
2. Drag (momentum reversal)- which acts parallel to the flow direction.

The blade rotation is nominally half that around the central shaft since this condition results in near optimum conditions for both lift and drag forces on each blade [9], but this is still under investigation and the exact details could be subjected to some changes. Figure 1 shows the rotation of the blade around the central axis presenting a variable incident angle to the flow during the rotation cycle. The power is taken off from the central shaft and transferred to a generator. The

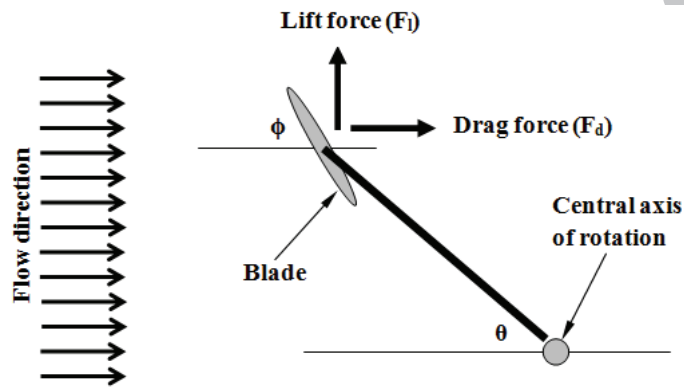


Figure 1: Torque on axis as a function of arm angle  $\theta$  and blade angle  $\phi$

blades are allowed to rotate about their own axis and also about a mutually central axis where the rotation axis is perpendicular to the flow direction in contrast to the better known windmill device. There are several aspects to this configuration which give it potential advantage particularly in water where the flow forces on the blades can be extremely high.

Since both the drag and lift exert forces, both of these can be used to extract energy from the fluid flow. Of these, lift has been the subject of considerably more attention since it is the basis of winged flight and also the basis for propeller based propulsion, whereas drag has been viewed as a problem to be overcome in this context. Nevertheless, for a given plate area and flow velocity, the drag force generally exceeds the lift force and is much less sensitive to the flow incident angle. The MRL turbine and its configuration is capable of taking advantage of both these characteristics through the operating cycle.

It is surprising that there is a set of blade conditions where both lift and drag forces act uni-rotationally around the main axis such that the torque contribution is positive over the whole cycle. This allows both lift and drag forces to act together to produce a large summed torque as described by [9].

Detailed CFD models of such machines (including blade geometry and blade motions) can be undertaken using dynamic (sliding) mesh or overset meshing techniques; however the ensuing calculations are computationally unrealistically expensive for more than a single turbine. Thus the use of simplified CFD based turbine modelling techniques becomes imperative for such turbines. In view of this, an empirically-based CFD model called the Immersed Body Force (IBF) model was developed based on the accepted methodology of the actuator disc but incorporating additional features that induce energy absorption from the flow so as to generate a downstream wake structure which more closely reflects that of the real turbines. This model could easily be made applicable to other turbine designs with few modifications. Some of the advantages of the IBF model include the capability of implementing drag and lift forces and the reduction of mesh resolution that is required compared to what would be required for a resolved blade simulation. This model has been used to analyse wake interactions of a small clusters of turbines as shown in [10–12]

Given that the long term goal of our work is to use the IBF model for large scale tidal farm modelling, it is important to validate the model's fidelity against experimental data. Therefore, the aim of this paper is: (i) to validate the accuracy of the IBF model for predicting the wake profiles of tidal turbines by comparing with experimental data measured from testing a scaled prototype of the MRL turbine; and (ii) to show that improved modelling techniques such as the IBF model could be developed for other specific turbine designs whilst maintaining their modelling simplicity and cheaper computational cost.

## 2. Methodology

### 2.1. Computational modelling

#### 2.1.1. Reynolds-averaged Navier-Stokes (RANS) modelling

The Navier-Stokes equations represent the equations of conservation of mass and momentum for a fluid in motion. However they are complex, coupled and non-linear, and thus insoluble analytically for anything but the simplest cases. For most realistic cases, computational solution using numerical methods, i.e. CFD, is the only practical approach. Particularly challenging is the solution of turbulent flow in a fluid. Turbulent flow is characterised by the presence of quasi-random

97 turbulent eddies on length- and time-scales ranging from large scales which drive  
 98 the turbulence down to the Kolmogorov scale determined by the physical viscosity.  
 99 For most practical cases direct numerical simulation of the complete range of  
 100 scales is impossible; instead the flow is decomposed into an ‘average’ component  
 101 and fluctuations about this average. The intention is that the average component is  
 102 smoother and computationally tractable, whilst the fluctuations are in some sense  
 103 universal and can be replaced by a simpler statistical model known as a turbulence  
 104 model. The Reynolds-averaged Navier-Stokes (RANS) equations are obtained in  
 105 this way by statistical averaging of the equations of motion, dividing the flow  
 106 into a deterministic mean flow which is steady or slowly varying and turbulent  
 107 fluctuations around this mean. The unsteady RANS modelling approach solves  
 108 the Reynolds averaged equations of mass and momentum conservation given in  
 109 Eqns: (1) and (2) respectively [7, 13]. The source term,  $F_b$ , represents the turbine’s  
 110 resistance force against the flow as discussed in section 2.1.3.

$$\frac{\partial U_i}{\partial x_i} = 0 \quad (1)$$

$$\frac{\partial U_i}{\partial t} + \frac{\partial U_i U_j}{\partial x_j} = -\frac{1}{\rho} \frac{\partial P}{\partial x_i} + \frac{\partial}{\partial x_j} \left[ \nu \left( \frac{\partial U_i}{\partial x_j} + \frac{\partial U_j}{\partial x_i} \right) \right] + \frac{\partial}{\partial x_j} \left( -\overline{U'_i U'_j} \right) + F_b \quad (2)$$

111 Where  $U$  is the Reynolds averaged velocity,  $P$  is the Reynolds averaged pressure;  
 112  $\nu$  is a kinematic viscosity, and  $\overline{U'_i U'_i}$  is the Reynolds stress tensor. The Reynolds  
 113 stress tensor is defined as:

$$-\overline{U'_i U'_i} = \nu_t \left( \frac{\partial U_i}{\partial x_j} + \frac{\partial U_j}{\partial x_i} \right) - \frac{2}{3} k \delta_{ij} \quad (3)$$

114 where  $k = \frac{1}{2} \overline{U'_i U'_i}$  is the turbulent kinetic energy, and  $\nu_t$  is the turbulent viscosity.

115 The Reynolds stress term,  $\overline{U'_i U'_i}$ , is modelled using the k-omega Shear Stress  
 116 Transport turbulence model ( $k\omega - SST$ ) [14]. The  $k\omega - SST$  turbulence model  
 117 has been used because of its capability of modelling separated flows.

### 118 2.1.2. Computational domain and inflow conditions

119 The dimensions of the computational domain are taken from the test tank facil-  
 120 ity with far upstream and downstream dimensions reduced to minimise the com-  
 121 putational cost as the experimental measurements were taken within this domain.



Details of the computational domain are shown in Figure 2. The size of the turbine relative to the size of the computational domain is very small and thus the turbine details is not clear. For this reason the turbine detail was scaled up by 10 times ( $10\times$ ) of the actual size as shown in Figure 2 so that all the dimensions and profile of the blades are visible. This means the dimensions of the blades shown in the figure should be scaled down by 10 in order to get their actual size. Different

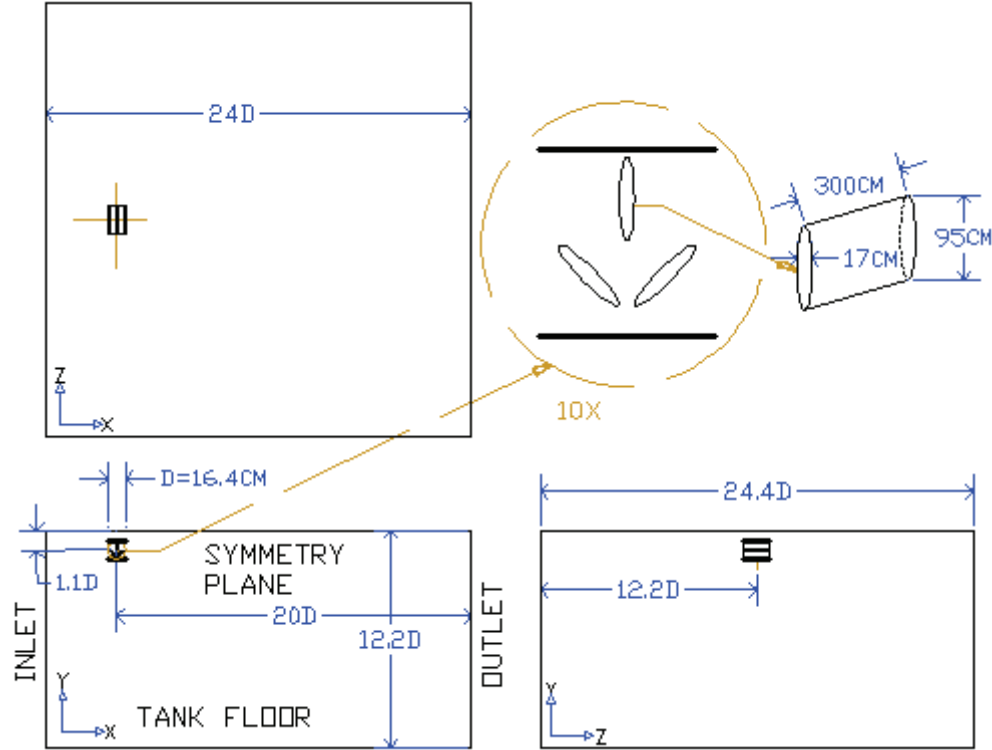


Figure 2: Dimensions of the computational domain

mesh resolution was used where the mesh was refined around the region of interest to resolve the shear layers while the rest of the region was slightly coarsened to decrease the computational cost. The resolution of the mesh was developed based on a mesh sensitivity study conducted by [11] on a different domain size with the turbine performance monitored to find mesh independent solutions.

The inflow conditions are required to be a realistic representation of the practical engineering situation, although sometimes it is difficult to achieve these conditions due to constraints such as time, cost and technology. In this study, the undisturbed flow profile of the test tank was established and the result shows that



the velocity slightly varies with depth. However, data was measured at a limited number of points across the depth of the channel and makes it difficult to directly use this data as inlet to the computational domain. The best option is therefore to apply an approximate tidal velocity profile developed by assuming a power law [15–17], which is matched to the experimental data as shown in Figure 3. The power law velocity profile gives good approximations for most tidal current sites and it can be estimated by assuming a power law of the form:

$$u(y) = u_{mean} \left( \frac{y}{0.32h} \right)^{1/9} \quad (4)$$

where:  $u_{mean}$  is the mean velocity,  $y$  is the vertical height, and  $h$  is the depth of water level.

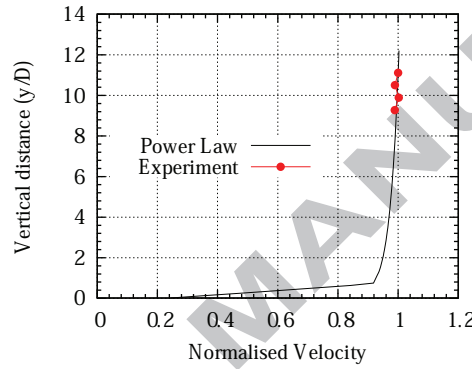


Figure 3: Matched experimental and Power law velocity profiles at the inlet to the computational domain.

The turbulence intensity was measured in the experiment and found to be around 3% and a similar value was prescribed at the inlet to the computational domain to replicate the actual conditions of the test tank. Computations were performed using the Open Source object-oriented C++ library, OpenFOAM, [18–20]. It uses Finite Volume Method solution technique in which the flow equations are volume-integrated over a discrete volume obtained by dividing the computational domain [20].

Tidal turbines may operate quite close to the water surface. However studies by [21–23] showed that the effect of the dynamics of the free surface on the wake profiles is minimal. In this study, the interest is on the wake profiles and thus modelling the free surface was excluded with a symmetry plane boundary condition used at the top of the computational domain instead of a more sophisticated multi-

158 phase technique such as Volume of Fluid (VoF). This also improved convergence  
159 of the simulations as VoF methods are much less stable than single phase models.

### 160 2.1.3. Turbine Modelling

161 Most researchers accept that simple momentum sink zone models such as the  
162 actuator disc methods are crude and make it difficult to incorporate energy loss  
163 processes. However, they are one of the few computationally realistic approaches  
164 for gaining insight into the behaviour of substantial clusters of devices. This study  
165 builds upon this accepted methodology by incorporating additional geometric fea-  
166 tures that induce energy absorption from the flow which also lead to a downstream  
167 wake structure intended to reflect more closely those of the real turbines than sim-  
168 ple momentum sink zone models. The turbine modelling method adopted for this  
169 study is therefore referred to as the Immersed Body Force (IBF) model, which is a  
170 novel turbine modelling technique developed by the authors of this paper [11, 23].  
171 The IBF model is capable of three roles:

- 172 1. Estimating the downstream wake structure.
- 173 2. Allowing calculation of the energy that can be extracted from the flow to-  
174 gether with a method of relating this to methods of estimating the useful  
175 power extracted by the turbine which can be validated against experiments.  
176 This typically requires access to a fully detailed CFD model as an interme-  
177 diate step.
- 178 3. Providing information about the free surface interaction. This is important  
179 in the class of machines considered here because they are designed to be  
180 deployed close to the surface, often supported by floating pontoons. Thus  
181 in principle pitch resonance of the pontoons could occur with undesirable  
182 results.

183 For the IBF approach, a forcing function ( $F_b$ ) which has units of force per unit  
184 mass representing the resistance by the turbine against the flow is used to create  
185 momentum change. The force function was imposed in the Navier-stokes equa-  
186 tions and a code was developed by considering drag ( $F_{RD}$ ) and lift ( $F_{RL}$ ) resis-  
187 tance forces applied by the blades on the fluid flow as shown in Figure 4. The  
188 forces are imposed on the volume of the blades and vortex ring which creates  
189 cylindrical shape to match design of the MRL turbine shown in Figure 5. This is  
190 different to the disc shape commonly used to represent the conventional axial type  
191 of tidal turbines.

192 The force applied by the vertical blade was considered entirely as a drag resis-  
193 tance force while the other two blades have both drag and lift resistance forces.

194 This force is a reaction force to the forces applied by the flow on the blades. The  
195 forcing function can be defined as:

$$F_b = F_{RD} + F_{RL} \quad (5)$$

196 The IBF model comprises two parts as shown in Figure 4:

- 197 1. A set of resistance forces seated on the cells corresponding to the fixed blade  
198 positions.
- 199 2. A force ring designed to represent the effect of the main turbine vortex .

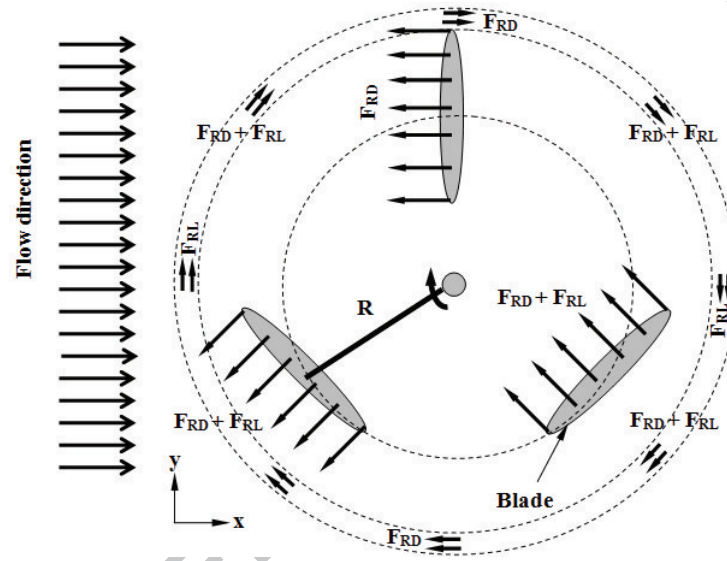


Figure 4: Body forces applied by each blade and annular section (*annular method*)

200 Both 1 and 2 contain the free parameters ( $F_{RD}$  and  $F_{RL}$ ) that define the associated  
201 resistances against the incoming flow. This type of representation has several  
202 advantages as summarised below:

- 203 • It reduces the requirement of mesh resolution at the surface because there  
204 is no physical presence of the blades in the model, which minimises the  
205 requirement of fine meshing to treat the blade surface and fluid interaction.
- 206 • It is applied in a volume which creates complex motions within the turbine  
207 housing

- The geometric features lead to downstream wake structures intended to reflect more closely those of the real turbines.
- If the physical blades were to use, they will be simply as solid boundaries imposing blockage but in the case of using the resistance forces, there is a flow of fluid through it similar to the porous region used in the application of actuator disc method. However, if excessive resistance were to be used, it will act as a blockage body similar to the physical body of the blades.
- It allows application of both drag and lift resistances against the flow based on the blade position.

Avoiding modelling the blade motions means that pressure integration over the blade surface cannot be used to directly calculate the mechanical power extracted by the machine from the flow. Consequently, published research on simplified descriptions of turbines of all kinds has focussed upon calculating the energy lost from the flow. Typical examples of this are the various developments of momentum sink models (e.g. actuator disc descriptions) or Darcy flow based models that implicitly represent the turbine by a viscous dissipation sink region. Examples of this approach are given in [3, 4, 6].

A similar approach has been undertaken in the work presented here. For this reason, it is difficult to utilise any loadings measured in the experiment directly to the CFD code as a resistance force because of the significant difference between the mechanical power absorbed by the machine and the total energy lost from the flow. The best approach is therefore to find a self consistent match of the flow profiles from the experiment and CFD by varying the loadings in the CFD calculations. This process can provide the necessary loading that can be used in the CFD code in order to predict the accurate wake recovery. With the correct loadings, CFD calculations can then be conducted to investigate the effect of wake interactions, and thus the location of individual devices in a tidal stream farm can be optimised to generate maximum power output. This approach is cost effective compared to full scale experimental works.

## 2.2. Experimental procedure

CFD simulations have been compared with experimental measurements of the MRL turbine conducted in a Wave-Current circulating tank (Figure 7a) at IFREMER, France. The tank's dimensions are 4 m wide, 2 m deep and 18 m in length.

An MRL turbine (Figure 5) with dimensions of 0.164 m diameter, 0.3 m blade span, and 0.095 m blade chord was used in the experiments. Two sided plates

243 were included in the design, one on the top and one on the bottom to increase the  
 244 Pelton and the ground effects, respectively.

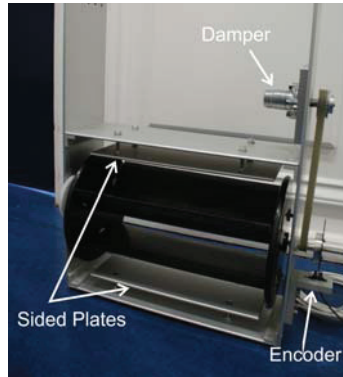


Figure 5: Momentum-Reversal-Lift type of horizontal axis tidal turbine

### 245 2.2.1. Calibration Procedure

246 The turbine load was provided by a dashpot system and a gear system that  
 247 connects the rotor and the dashpot. The gear ratio used in the experiments was  
 248 12-24. The damping was provided by the viscous fluid contained in the dashpot  
 249 with a viscosity of 250,000 cst.

250 The calibration was carried out with a torque rig composed of a contactless ro-  
 251 tary torque transducer rated at 2 Nm, a hall effect sensor and a Crouzet DC Motor.  
 252 The motor was used to rotate the damper at various angular velocities while the  
 253 torque transducer measured the torque generated by the damper. Figure 6 shows  
 254 the calibration obtained for the dashpot used during the experiments presented in  
 255 this work.

256 It can be observed that the dashpot behaves noticeably different from the char-  
 257 acterisation given by the manufacturer. Thus the need to carry out a pre and post  
 258 calibration was imminent. The standard deviation analysis gave a maximum vari-  
 259 ation value of 0.01 Nm when calibrating the damper. With the calibration, a poly-  
 260 nomial approximation relating torque and angular speed was obtained and used  
 261 to calculate the torque developed by the turbine at the angular speed measured  
 262 during the experiment. The torque was then inferred from the angular speed mea-  
 263 sured with the same type of hall effect sensor used in the calibration procedure.  
 264 Hence power extracted was estimated from the rotational velocity only.

265 As this turbine was specially designed to be utilised in shallow-medium flow  
 266 estuaries, the turbine was installed very close to the surface of the Wave-Current

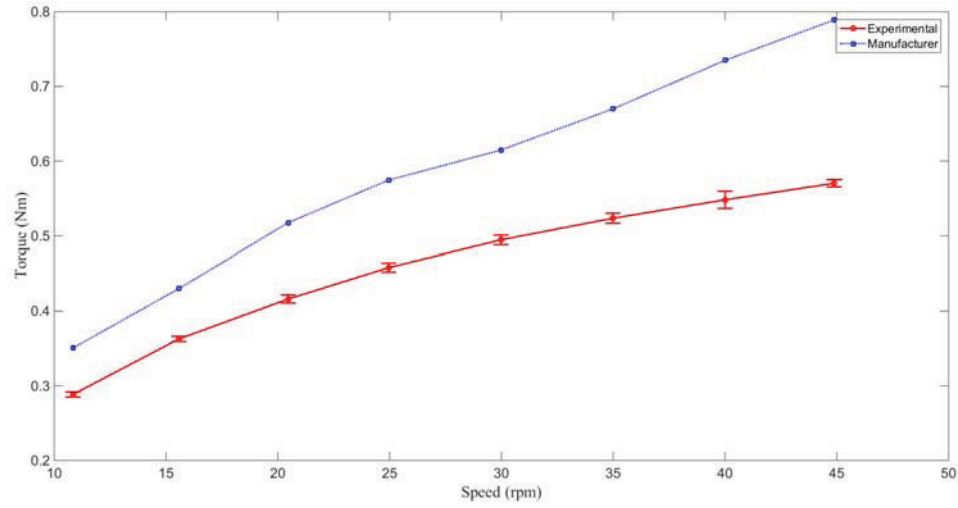


Figure 6: Relation of torque and speed of a dashpot with viscosity of 250 kcs

267 circulating tank. The distance between the main shaft and water surface was set  
 268 to 1.1D, as seen in Figure 2. The turbine was rigidly mounted on the top of the  
 269 tank using H-beams available at the facility as shown in Figure 7a. The turbine  
 270 was held in place by an aluminum frame that was previously anodised to avoid or  
 271 diminish corrosion problems.

#### 272 2.2.2. Flow measurements

273 The turbine was operated in a flow regime of 1.0 m/s with a turbulence inten-  
 274 sity of around 3%. The wake generated by a single MRL turbine was characterised  
 275 by measuring velocity components at a range of points downstream of the turbine.  
 276 A 2D laser Doppler velocimeter (LDV), mounted on a computer-controlled gantry  
 277 was used to measure velocity at a large number of points downstream of the tur-  
 278 bines, thus building up 'velocity grids'. The velocity grids are represented by  
 279 two velocity components  $x$ , and  $z$ . The  $x$  velocity component is the streamwise  
 280 component and the  $z$  velocity vector is the downward component. The number  
 281 of velocity points measured in this experiment was 420. 15 downstream wake  
 282 planes (along the  $X$  direction) were measured during the trials (-2D, -1.5D, -1D,  
 283 1D, 1.5D, 2D, 2.5D, 3D, 3.5D, 4D, 6D, 8D, 10D, 15D and 20D). Velocity at each  
 284 node was measured for 100s.

285 Figure 7b shows the LDV probe during operation. The velocity grids on the  
 286 cross-sectional area were limited to measurements from the main turbine shaft



(a) Top view of the tank  
(b) LDV probe

Figure 7: Experimental facility at IFREMER, France

and vertically towards the tank bottom. The reason behind this was due to water reflections affecting the measurements if the LDV probe operated very close to the water surface.

### 3. Results and Discussions

#### 3.1. Load variations

The experimental measurement of the flow characteristics was carried out at the MRL turbine's nominal power output. In order to match this experimental data, CFD simulation using the RANS + IBF model was conducted with different loadings. All the loadings were normalised by the maximum loading applied in this particular case for simplicity purposes and is defined as  $NBF = F_b/F_{bmax}$ . This notation is used for subsequent discussions to identify the loadings for each case.

The velocity contours from the three different loadings are shown in Figure 8. The effect of different loadings on the flow characteristics is visible immediately downstream of the turbine but needs detailed data extraction from the velocity contours for more clarification of the flow profiles among the different loadings as discussed in section 3.2.

#### 3.2. Flow field analysis

Detailed velocity data was extracted in the stream-wise direction through the center of the turbine to understand the rate of wake recovery from the CFD +



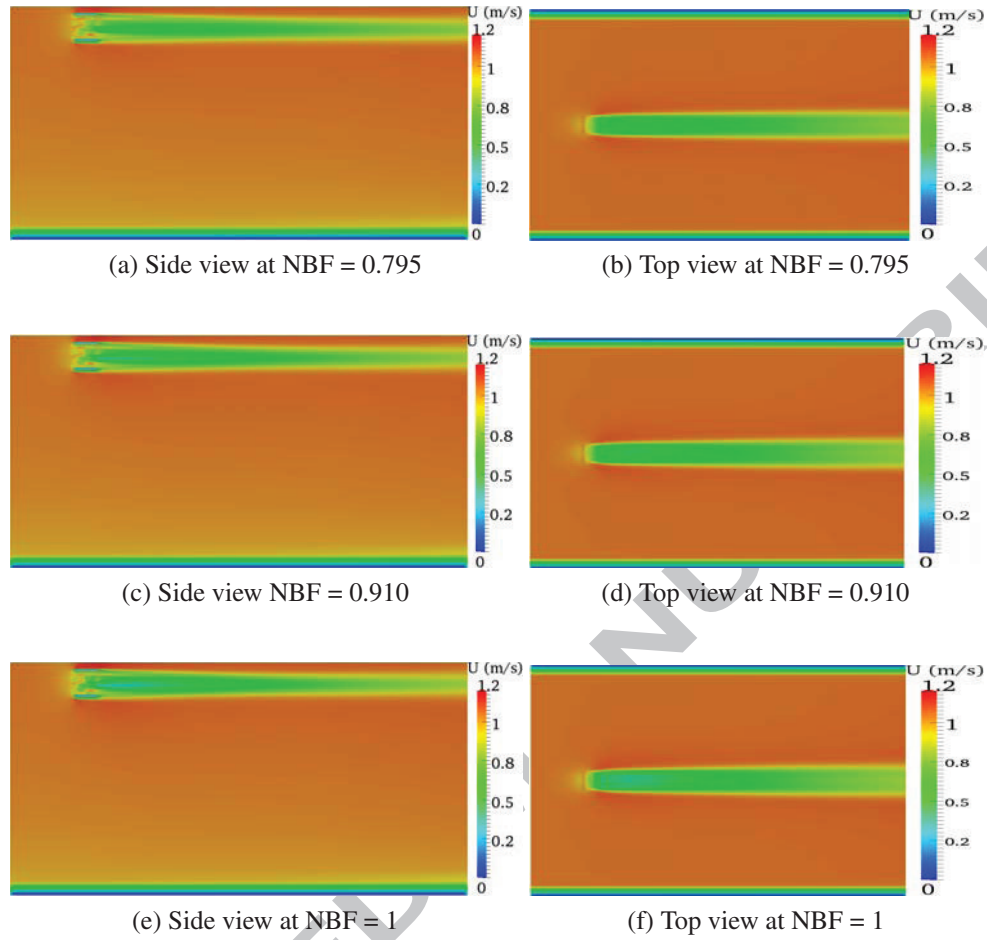


Figure 8: Snapshots of velocity contours of the tidal turbine at different loadings

IBF model and to get the best match with the experimental data as shown in Figure 9. At higher loading ( $NBF = 1$ ), there is huge velocity deficit immediately downstream of the turbine but the wake recovers faster than is the case for lower loadings. This has a profound effect in building optimised tidal stream farms because of the effect of wake interactions on performance of downstream devices thus finding the loading with the best match to the experiment is crucial for large scale tidal farm simulations.

At lower loading ( $NBF = 0.795$ ), the velocity deficit at the turbine region is smaller but recovers at a slower rate and shows better match with the experimental

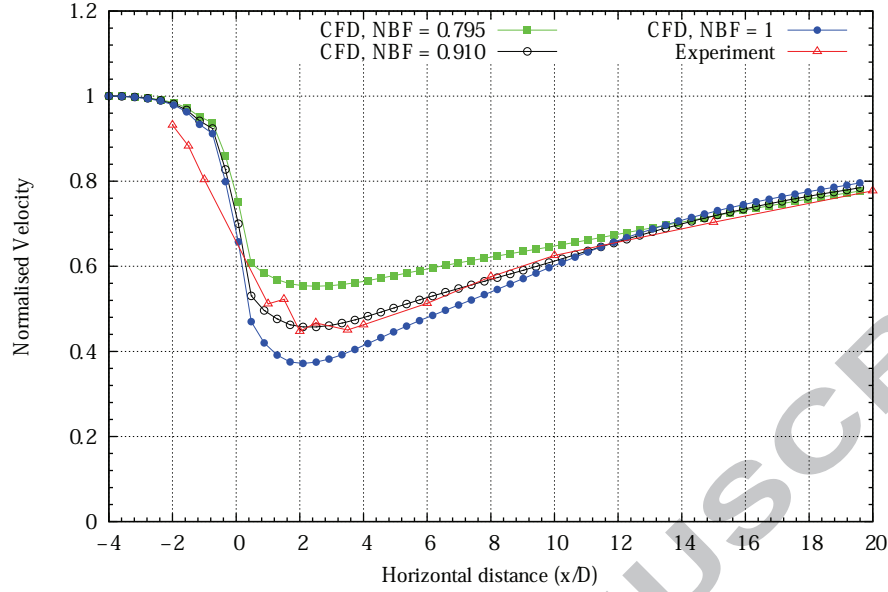


Figure 9: Experimental and CFD comparisons of the Span-wise flow profiles through the centre-line of the turbine

data further downstream of the turbine from 15D onwards. The CFD predictions with the loading ( $NBF = 0.910$ ) showed good match between 0D and 13D compared to the other loadings but is inconsistent throughout the velocity profile. The CFD results show that the rate of wake recovery is faster with higher loadings though it is difficult to show the same trend in the experimental data as the existing measurements are from a single loading. The trend from those calculations indicate that any value above the maximum and below the minimum loadings applied in these calculations will deviate significantly from the experimental data though further higher loading could produce a better match with the experiments upstream of the turbine.

For further analysis of the wake profiles along the depth of the domain, measurements were performed at different points during the experiment and similar data was extracted from the CFD calculations at  $NBF = 0.910$ , the loading which showed the best match with the experimental data. The effect of the turbine in the upstream flow from -4D to 0D is higher in the experiment compared to the CFD results leading to big difference in the flow profiles as shown in Figure 10. One of the possible reasons for this difference is that in the case of the MRL turbine, rotation of the blades is perpendicular to the fluid flow which increases the

blockage effect on the upstream flow compared to the commonly used traditional tidal turbines where their blade rotation is parallel to the flow. This huge blockage effect by the MRL turbine doesn't seem to be sufficiently replicated by the CFD modelling. However, it is clear to see that the higher loading has more effect on the upstream flow compared to the lower loadings in the CFD calculations as shown in Figure 9.

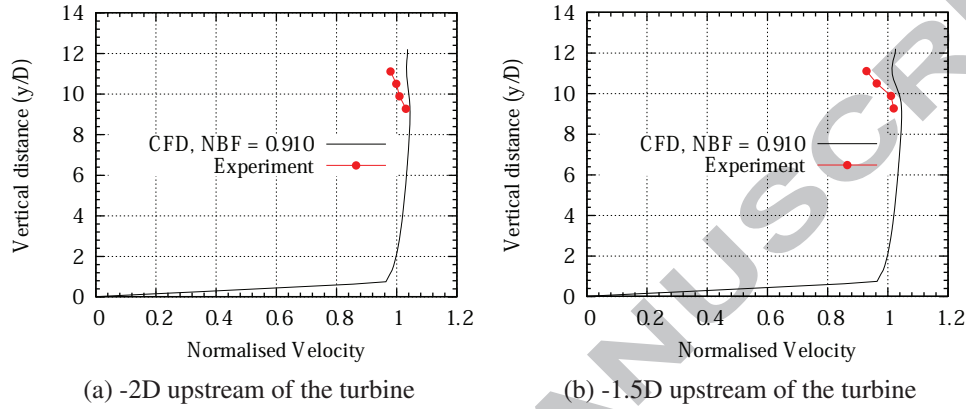


Figure 10: Comparisons of the upstream vertical velocity profiles of the CFD calculations at NBF = 0.910 and experimental data

The vertical velocity profiles of the downstream wake in Fig 11 showed reasonable agreement, which is consistent with the stream-wise flow profiles discussed in Figure 9.

However, there are some noticeable differences in these vertical velocity profiles. The wake expansion from the CFD results is slightly wider from 1D to 2D (Figs. 11a - 11c) and narrower from 8D onward while they are almost similar at the transition phase from 4D to 6D. The rate of wake recovery in the vertical profiles reflects the same trend as the stream-wise velocity profiles discussed in Figure 9.

These inconsistencies are an indication of the limitations of the RANS + IBF calculations in predicting the realistic flow conditions of the experimental data. Since the IBF model is developed on the notion of non-rotating blades, this clearly has some limitations compared to detailed CFD modelling techniques. Those limitations are mostly related to the way the energy is extracted from the flow plus the swirling type of flows that are produced by rotating turbines.

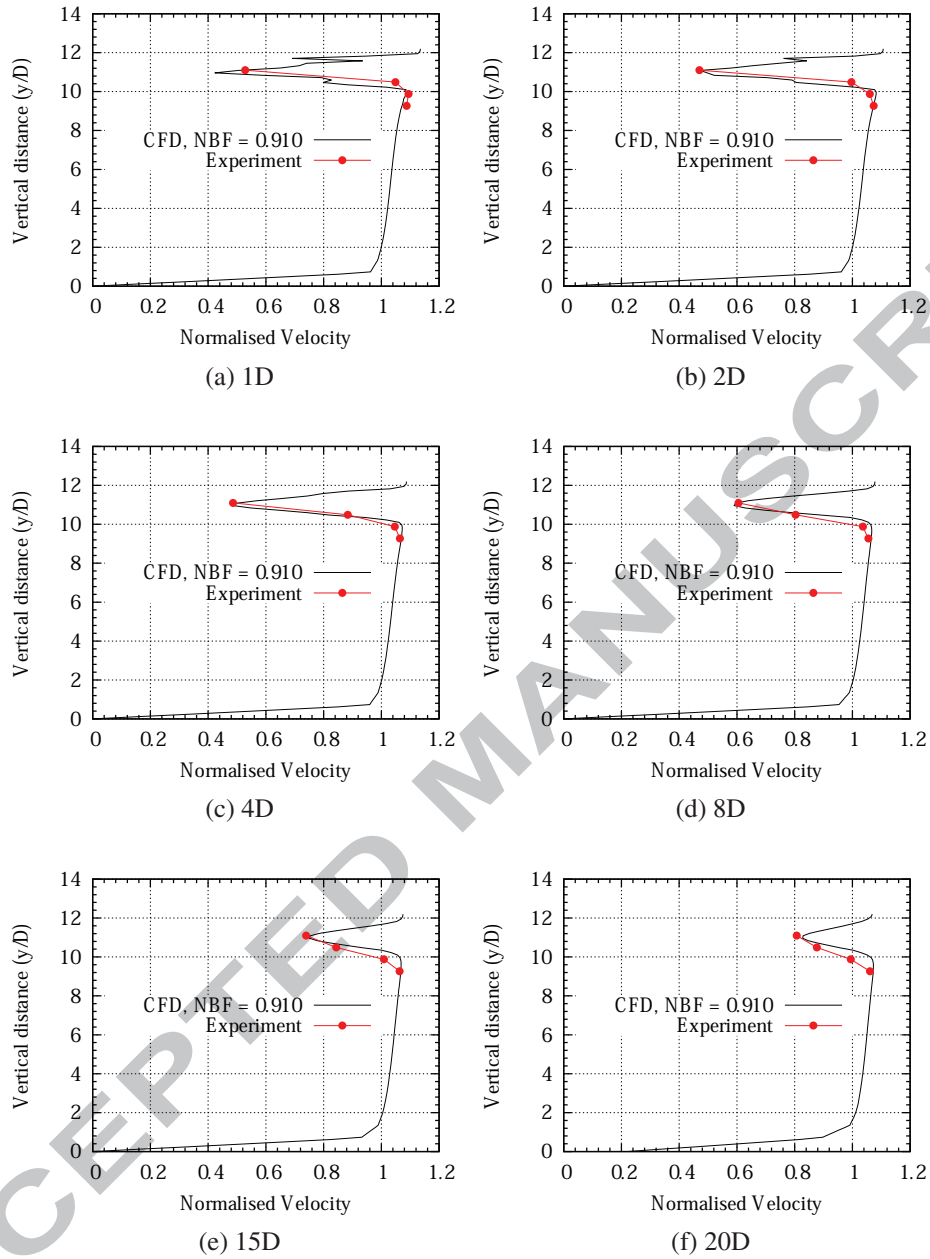


Figure 11: Comparisons of the wake vertical velocity profiles of the CFD calculations at NBF = 0.910 and experimental data

### 3.3. *Execution time of the simulations*

The simulations were carried out using an 8 GB machine. Detailed 2D CFD simulations of the MRL turbine using dynamic sliding mesh takes more than 240 hours for 20 revolutions of the blades (to obtain fully developed wake structure). The 2D simulations of the MRL turbine was conducted as part of the EPSRC funded project but was computationally very expensive and thus 3D simulations was not conducted. In the case of the IBF model, simulation of a single turbine takes about 8 hours to obtain fully developed wake structures which is much cheaper than the detailed CFD model even for 3D CFD simulations. Though it is obvious that the two are not directly comparable, it is clear to see the magnitude of their difference in the simulation time. Practically 2D simulation is computationally cheaper than 3D simulations but still the 2D simulations using dynamic sliding mesh method is 30 times higher than the 3D simulations using the IBF model. This is because CFD model with a physical presence of the blades can significantly increase the computational power due to the treatment involved to resolve the flow on the surface of the blades. However, in the case of the IBF model, there is no physical presence of the blades as discussed in the previous sections which resulted in cheaper computational cost.

## 4. Conclusion

The empirically-based IBF model developed based on the concept of the actuator disk method was calibrated against flow characteristics data for an MRL turbine obtained from experiment in the IFREMER Wave-Current circulating tank, France. The model was found to perform well, although we recognise that it does not necessarily fully reproduce all the large scale deterministic flow patterns in the way that a dynamic blade motion simulation would do. This was reflected in some of the inconsistency observed on the flow profiles between the CFD and experimental data. However such a blade motion simulation would be in the orders of magnitude more expensive to calculate, and the IBF method is thus computationally cheap enough to allow multiple turbine simulations to be run. Therefore, considering the complexity and computational cost of modelling a detailed blade motion the limitations of the IBF model are acceptable and will be useful especially for optimisation of arrays of devices where there is a significant computational demand.

## Acknowledgement

We would like to thank EPSRC for providing the funding under project number EP/J010138/1, as part of the Supergen Marine research program and the IFREMER personnel of Boulogne-sur-Mer for their assistance and advice during the experimental trials.

## Bibliography

- [1] S. Gant and T. Stallard. Modelling a tidal turbine in unsteady flow. In *Proceedings of the Eighteenth (2008) International Offshore and Polar Engineering Conference*, pages 473–479, 2008.
- [2] ME Harrison, WMJ Batten, LE Myers, and AS Bahaj. Comparison between CFD simulations and experiments for predicting the far wake of horizontal axis tidal turbines. *Renewable Power Generation, IET*, 4(6):613–627, 2010.
- [3] R. Mikkelsen. *Actuator disc methods applied to wind turbines*. PhD thesis, Technical University of Denmark, 2003.
- [4] B. Sanderse. Aerodynamics of wind turbine wakes. *Energy Research Center of the Netherlands (ECN), ECN-E-09-016, Petten, The Netherlands, Tech. Rep*, 2009.
- [5] C.S.K. Belloni and R.H.J. Willden. Flow field and performance analysis of bidirectional and open-centre ducted tidal turbines. In *9th European Wave and Tidal Energy Conference*, 2011.
- [6] AJ MacLeod, S. Barnes, KG Rados, and IG Bryden. Wake effects in tidal current turbine farms. In *International Conference on Marine Renewable Energy-Conference Proceedings*, pages 49–53, 2002.
- [7] X. Sun, JP Chick, and IG Bryden. Laboratory-scale simulation of energy extraction from tidal currents. *Renewable Energy*, 33(6):1267–1274, 2008.
- [8] William MJ Batten, ME Harrison, and AS Bahaj. Accuracy of the actuator disc-rans approach for predicting the performance and wake of tidal turbines. *Philosophical Transactions of the Royal Society of London A: Mathematical, Physical and Engineering Sciences*, 371(1985):20120293, 2013.

- 417 [9] A.P. Janssen and M.R. Belmont. Initial research phase of MRL turbine. Tech-  
418 nical report, Technical Report N0:MO 562L, 2009.
- 419 [10] Muluaem G Gebreslassie, Gavin R Tabor, and Michael R Belmont. Cfd  
420 simulations for sensitivity analysis of different parameters to the wake char-  
421 acteristics of tidal turbine. *Open Journal of Fluid Dynamics*, 2:56, 2012.
- 422 [11] Muluaem G Gebreslassie, Gavin R Tabor, and Michael R Belmont. Investi-  
423 gation of the performance of a staggered configuration of tidal turbines using  
424 cfd. *Renewable Energy*, 80:690–698, 2015.
- 425 [12] Muluaem G Gebreslassie, Gavin R Tabor, and Michael R Belmont. Numer-  
426 ical simulation of a new type of cross flow tidal turbine using openfoam–  
427 part ii: Investigation of turbine-to-turbine interaction. *Renewable Energy*,  
428 50:1005–1013, 2013.
- 429 [13] ME Harrison, WMJ Batten, and AS Bahaj. A blade element actuator disc  
430 approach applied to tidal stream turbines. In *OCEANS 2010*, pages 1–8.  
431 IEEE, 2010.
- 432 [14] FR Menter, M Kuntz, and R Langtry. Ten years of industrial experience with  
433 the sst turbulence model. *Turbulence, heat and mass transfer*, 4(1), 2003.
- 434 [15] H. Schlichting and K. Gersten. *Boundary-layer theory*. Springer, 2004.
- 435 [16] F.M. White. *Viscous fluid flow*, volume 66. McGraw-Hill New York, 1991.
- 436 [17] WMJ Batten, AS Bahaj, AF Molland, and JR Chaplin. The prediction of the  
437 hydrodynamic performance of marine current turbines. *Renewable energy*,  
438 33(5):1085–1096, 2008.
- 439 [18] H. Jasak, A. Jemcov, and Z. Tukovic. Openfoam: A c++ library for com-  
440 plex physics simulations. In *International Workshop on Coupled Methods in*  
441 *Numerical Dynamics, IUC, Dubrovnik, Croatia*, 2007.
- 442 [19] H. Jasak. Multi-physics simulations in continuum mechanics. In *Proceed-*  
443 *ings of 5th International Conference of Croatian Society of Mechanics, Tro-*  
444 *gir*, page, 2006.
- 445 [20] Henry G Weller, G Tabor, Hrvoje Jasak, and C Fureby. A tensorial ap-  
446 proach to computational continuum mechanics using object-oriented tech-  
447 niques. *Computers in physics*, 12(6):620–631, 1998.



- 448 [21] GT Houlsby, S Draper, MLG Oldfield, et al. Application of linear momen-  
449 tum actuator disc theory to open channel flow. *Report no. OUEL*, 2296(08),  
450 2008.
- 451 [22] ME Harrison. *The accuracy of the actuator disc-RANS model for predicting*  
452 *the performance and far wake of a horizontal axis tidal stream turbine*. PhD  
453 thesis, University of Southampton, 2011.
- 454 [23] Mulualem G Gebreslassie. *Simplified CFD modelling of tidal turbines for*  
455 *exploring arrays of devices*. PhD thesis, University of Exeter, 2012.